

Conductive Metal–Organic Framework Thin Film Hybrids by Electropolymerization of Monosubstituted Acetylenes

Svetlana Klyatskaya,* Anemar Bruno Kanj, Concepción Molina-Jirón, Shahriar Heidrich, Leonardo Velasco, Carsten Natzeck, Hartmut Gliemann, Stefan Heissler, Peter Weidler, Wolfgang Wenzel, Carlos Cesar Bof Bufon, Lars Heinke,* Christof Wöll, and Mario Ruben*



Cite This: *ACS Appl. Mater. Interfaces* 2020, 12, 30972–30979



Read Online

ACCESS |



Metrics & More

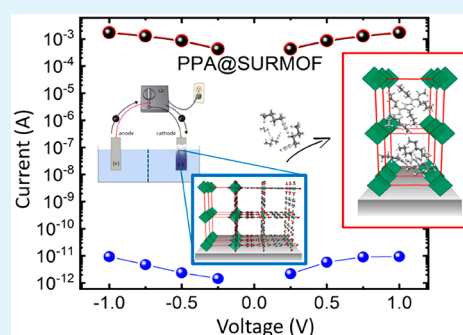


Article Recommendations



Supporting Information

ABSTRACT: 1-Hexyne monomers were potentiostatically electropolymerized upon confinement in 1D channels of a surface-mounted metal–organic framework Cu(BDC) (SURMOF-2). A layer-by-layer deposition method allowed for SURMOF deposition on substrates with prepatterned electrodes, making it possible to characterize electrical conductivity in situ, i.e., without having to delaminate the conductive polymer thin film. Successful polymerization was evidenced by mass spectroscopy, and the electrical measurements demonstrated an increase of the electrical conductivity of the MOF material by 8 orders of magnitude. Extensive DFT calculations revealed that the final conductivity is limited by electron hopping between the conductive oligomers.



KEYWORDS: monosubstituted acetylenes, MOF thin film, confinement in 1D channels of SURMOF, electropolymerization, conductivity

1. INTRODUCTION

Electrochemical polymerization (EP) via oxidation or reduction of organic precursors has become one of the key methods in nanoscience.^{1–3} This powerful tool enabled the development of modified electrodes that extended the panel of new conducting polymer-based materials, such as electrogenerated composites^{4,5} and led to numerous new applications, ranging from energy conversion and storage⁶ and electrocatalysis⁷ to electrotriggered drug delivery⁸ and biocompatible films.⁹ Moreover, EP can be performed under galvanostatic, potentiostatic, or most commonly potentiodynamic conditions,¹⁰ and represents a useful method to synthesize conducting polymers in the form of thin films from a number of different aromatic monomers (pyrrole, thiophene, and aniline).^{11,12} Polyacetylene (PA) is one of the original and best-known π -conjugated polymers, which bears one of the simplest repeating units $(-\text{HC}=\text{CH}-)_n$. In previous works, free-standing polyacetylene films have been electrochemically synthesized using anodic or cathodic condensation of acetylene in aprotic media.^{13–15} The electrochemical method has been proven to be an effective technique to fabricate porous molecular conductors (PMCs)—electroactive frameworks, which exhibit porosity, a through-space conduction pathway, and a high density of charge carriers (electrons). In previous works, synthesis was performed by electrocrystallizing of Cd^{2+} and N,N' -di(4-pyridyl)-1,4,5,8-naphthalenetetracarboxydiimide (NDI-py).¹⁶

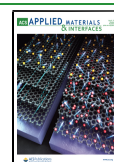
Metal–organic frameworks (MOFs) are a very rich class of materials with considerable potential, such as, for example, catalysts and adsorbents.^{17,18} Beyond these more traditional applications, there is an emerging interest in utilizing the electrical and optical properties of this rich class of materials to fabricate sensors and electronic devices,¹⁹ including photovoltaics.²⁰ At present, however, this potential is severely limited by difficulties in rendering sufficiently high electrical conductivity to these porous materials.²¹ Previously, two examples related to the loading of redox active molecules into the pores of the MOFs have been reported.^{22,23} Alternatively, an increase in electrical conductivity upon in situ polymerization within the pores of bulk MOFs was reported for confined monomers of pyrrole (Pyr) and thiophene (Th).^{24,25}

Moreover, nanochannels of MOFs have proven to be desirable fields, not only for the precision synthesis of polymer materials but also for exploring specific properties of polymer confinement, thus offering a unique tool toward controlled synthesis of confined polymers.²⁶ MOF-based composites with enhanced electrical conductivity can also be attained through efficient compositing of MOFs with conductive components

Received: April 21, 2020

Accepted: June 8, 2020

Published: June 23, 2020



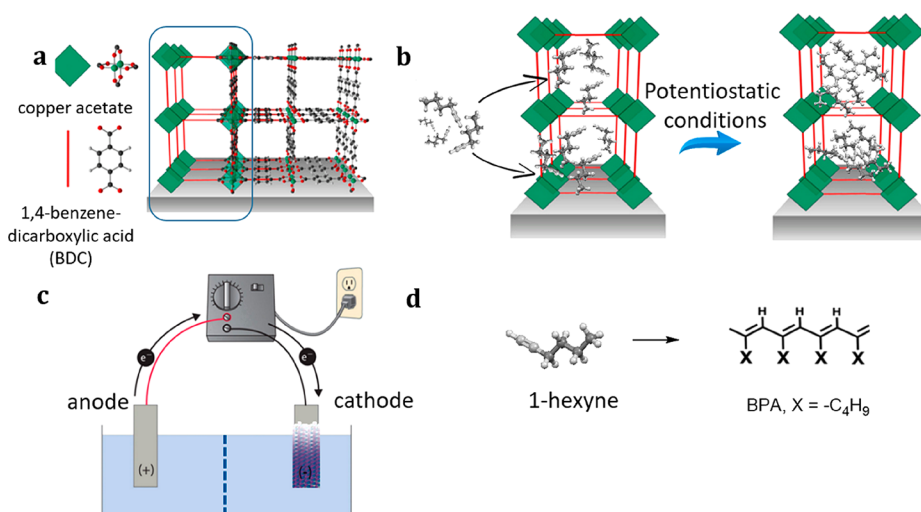


Figure 1. Schematic presentation of the use of Cu(BDC) SURMOF-2 as working electrodes in an electrochemical cell. (a) Side view of Cu(BDC) crystal structure grown along the [001] direction on a MHDA SAM. In red, oxygen; in green, copper; in black, carbon. (b) Scheme showing the encapsulation of alkyne monomer and the polymer formation inside the nanochannels of SURMOF-2. (c) Schematic representation of the electrochemical cell. (d) Scheme of polymerization of monosubstituted alkyne (1-hexyne, C₆H₁₀).

such as graphene.^{27,28} These previous examples, however, have been reported for the bulk form of MOF materials, which make reliable characterization of electrical properties somewhat difficult. For highly reproducible measurements, MOF thin films grown on conducting, patterned substrates are much better suited. So far, however, the polymerization inside such thin layers has been restricted to a few cases of SURMOFs (surface mounted metal organic frameworks) where monomers of 3,4-ethylenedioxythiophene (EDOT) could be polymerized to yield (electrically nonconducting) polythiophene oligomers.²⁹ Considering that in previous work polymerization of monomers embedded in MOFs has been studied in quite some detail,^{30,31} it is surprising that, to the best of our knowledge, there is only one previous report³² on electropolymerization of monomers embedded in MOFs. In this pioneering work, HKUST-1 thin films supported on a polyaniline substrate were utilized as template for the electrochemical synthesis of a microporous conductive polyaniline polymer. In this case, however, the conductivity could not be determined in situ, but only after delamination and further processing of the product.

2. RESULTS AND DISCUSSION

Here, we focus on the electrochemical synthesis and in situ characterization of a different conductive, polymer, polyacetylene (PA). PA is a particular attractive compound because this material exhibits the highest electrical conductivity³³ among polymers. We describe the electropolymerization of a monosubstituted alkyne, namely 1-hexyne, to afford butyl-substituted polyacetylene (BPA). As host MOFs we used Cu(BDC)-SURMOF-2 (BDC = 1,4-benzenedicarboxylate) grown on functionalized Au@SiO₂ substrates using a layer-by-layer (lbl) technique. After loading the monomers inside the 1D channels of the host framework we used potentiostatic electropolymerization to synthesize BPA chains embedded in the 1D-channels of the MOF thin film. The use of the lbl technique to grow the SURMOFs allowed us to characterize the electrical conductivity of the product in situ, revealing a huge increase in electrical conductivity. The resulting BPA@

SURMOF-2 composite thin films exhibited values of 8 orders of magnitude larger than for the pristine SURMOF.

A particular advantage of the SURMOF-based approach presented here is that it provides a convenient way to fabricated polyacetylene thin films by avoiding the severe problems (polyacetylene is insoluble in solvents) of preparing thin films of this material using, for example, spin coating. The chemical and physical properties of substituted PAs are strongly related to the structure of their main chains.^{34–36} 1-Hexyne was chosen as monomer to establish the occurrence of electroinitiated polymerization through C≡C bonds. To make EP processes occur efficiently and reproducibly within MOFs, we need stable, preferentially monolithic MOF thin films rigidly anchored to an electrode. A number of different methods to produce MOF coatings have been developed.²⁰ For the intended application in the context of the work presented here, it would be beneficial to use oriented MOF thin films, considering the potential application on novel hybrid electric and electronic devices.³⁷ In this context, SURMOFs carry a particular potential, because they can be grown in a layer-by-layer (lbl) fashion on appropriately functionalized substrates, yielding highly oriented monolithic thin films. We have chosen the Cu(BDC) SURMOF-2 formed by Cu paddle-wheel metal nodes connected by 1,4-benzenedicarboxylic acid (BDC) linkers deposited on top of a MHDA-SAM (mercaptohexadecanoic acid self-assembled monolayer).³⁸ A layer-by-layer process described previously^{20,39,40} was used to obtain monolithic, oriented films with channels within the MOF-layer running parallel to the surface. Cu(BDC) SURMOF-2 exhibits *P4* symmetry³⁸ and forms 1D channels, propagating along the crystallographic [001] direction (Figure 1a).

As a first step with regard to the fabrication of polyacetylene thin films, the pores of SURMOF-2 were loaded with 1-hexyne by immersion of the MOF-coated substrates into a solution of the 1-hexyne monomers in dry dichloromethane. The presence of 1-hexyne guest molecules inside the framework after 10, 25, and 45 h of immersion was monitored by Raman spectroscopy (Figure S1). The loading of the monomer is evident by the increase in the Raman peaks at 2930 cm⁻¹, assigned to the C–

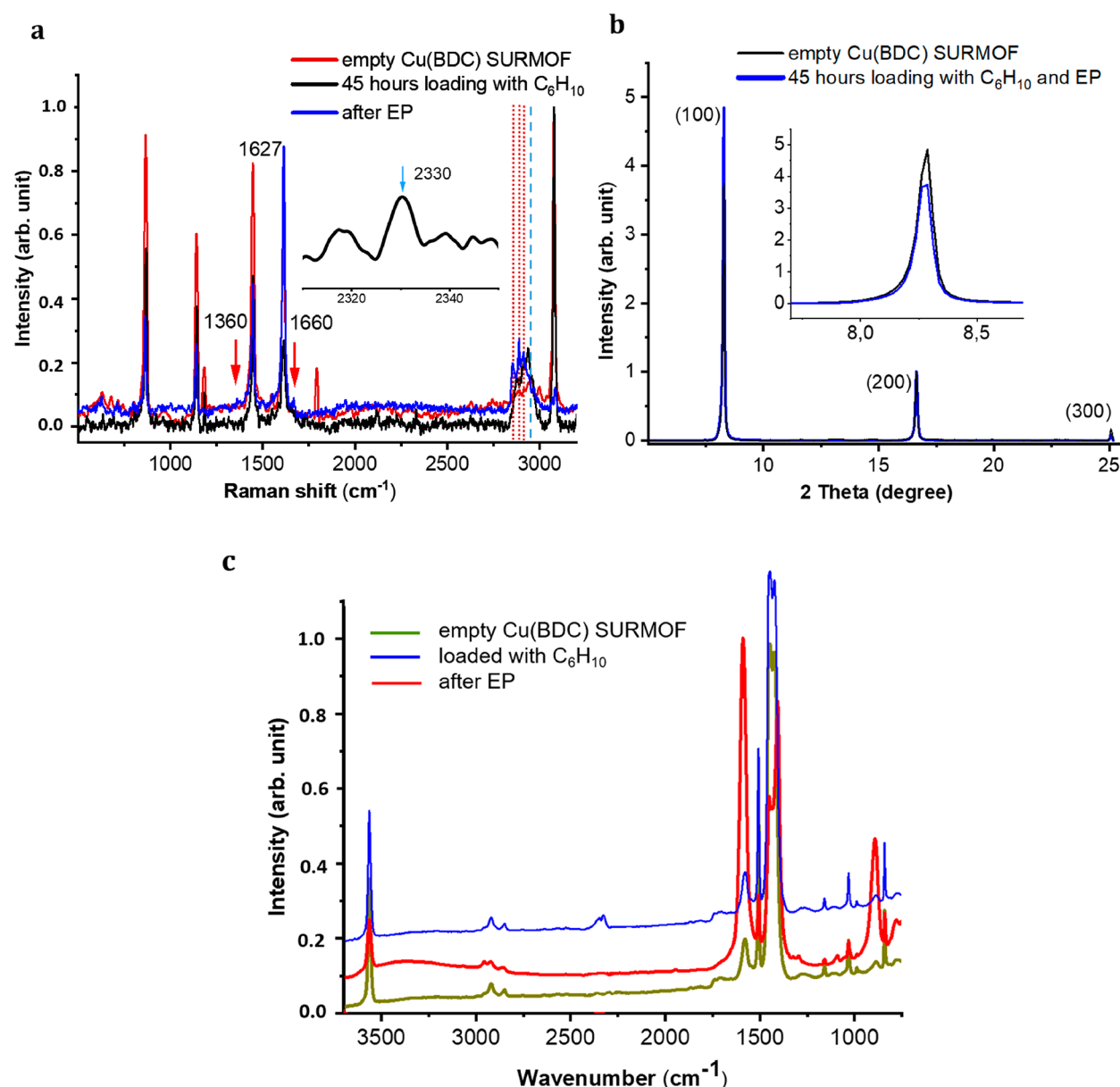


Figure 2. Monitoring of the electropolymerization process. (a) Raman spectra monitoring the evaluation of the morphological changes upon EP. (b) Out-of-plane X-ray diffractogram for the SURMOF film prior and subsequent 1-hexyne loading and electropolymerization (normalized to [200]). (c) IRRAS spectra of Cu(BDC) SURMOF-2 film before and after EP (with offset for better visibility).

H stretches⁴⁰ of butyl-tails of 1-hexyne monomer, and at 2330 cm^{-1} , assigned to $\text{C}\equiv\text{C}$ triple bond stretches (Figure 2a) that are shifted to higher energy in comparison with the net compound and matched quite well with our simulated Raman frequencies extracted from the DFT calculations, as shown in Figure S9. This type of phenomenon has been reported for the coordination of alkynes to metal ions and nanoparticles.^{41,42} The $\text{C}\equiv\text{C}$ stretches at around 2300 cm^{-1} are visible in the IR spectrum and provide quite strong evidence for a change in the molecular dipole of the confined triple bond.⁴³ XRD measurements carried out after immersion showed no major differences to those recorded for the pristine film (Figure S2).

The absence of a change in form factor is expected because loading 1-hexyne molecules into the pores of SURMOF-2 leads to only small changes in the electron density. To determine the polymer geometries in the pore, we performed DFT geometry optimizations, revealing as the most probable

scenario a modified conformation based on the trans–transoid form, shown in Figure S11, in which the alternating $-\text{C}_4\text{H}_9$ groups were rotated around the backbone by approximately 30° away from their neighbors. Subsequently, the 1-hexyne-loaded thin films were immersed in 1-hexyne-free dichloromethane solution with 0.1 M tetrabutylammonium hexafluorophosphate (TBAHFP) as a supporting electrolyte. Then, a negative voltage was applied to initiate the electropolymerization process (Figure 1). The polymer chain formation process is depicted schematically in Figure 1d and is associated with the formation of BPA. Prior to the potentiostatic EP experiments and in order to evaluate the range of working potential, we have characterized the electrochemical properties of loaded SURMOF-2 samples by means of cyclic voltammetry (CV). The CV was performed using standard electrochemical equipment under an argon atmosphere in dry dichloromethane containing 0.1 M TBAHFP as supporting electrolyte at a scan

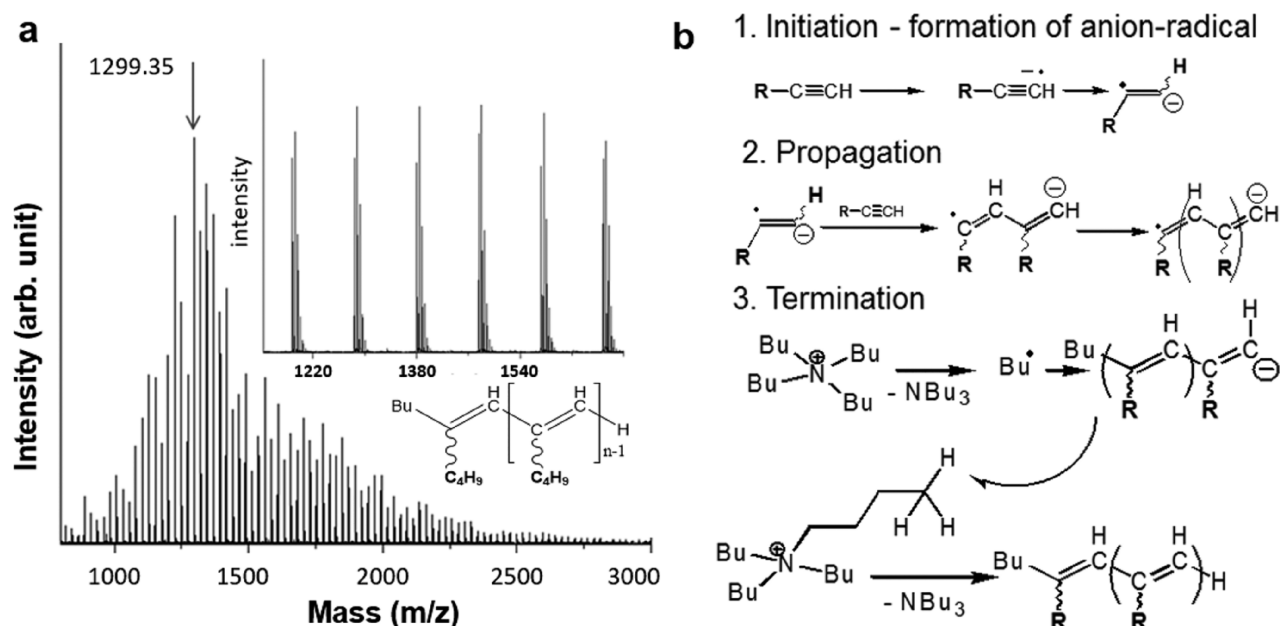


Figure 3. Proposed convergent-reaction pathways. (a) MALDI-ToF MS spectrum of BPA after dissolution of SURMOF-2 framework in acetic acid/ethanol (inset: partially enlarged spectrum). (b) Proposed mechanism of the electro-initiated polymerization through $C\equiv C$ bonds.

rate of 50 mV s^{-1} at RT, in contact to 20 mM 1-hexyne, or without it, for reference tests (Figure S3, see the [Supporting Information](#)). In the blank experiments, the SURMOF coating rather effectively blocks the charge flow through the film, as reported in previous work.²¹ Moreover, in contrast to the cyclic voltammetric behavior of the Cu(I)-ions containing solutions,¹⁴ no evidence of redox processes associated with Cu from the paddlewheel metal node could be observed. For the 1-hexyne-loaded samples, the CVs showed pronounced differences, and a substantial current density of 10 mA cm^{-2} was observed. There was an oxidation peak of 1-hexyne during the first anodic scan on the cyclic voltammogram (Figure S3), which can be attributed to the oxidative homocoupling process at the ethynyl substituents. The cathodic scan revealed the appearance of two irreversible reduction peaks at -1.25 and -1.60 V (versus Ag/Ag⁺). We assign the higher voltage peaks to the formation of the initial radical anion, the first step of the polymerization process. The peak at lower voltages has been assigned to the subsequent propagation step, where the initial radical anion reacts with a molecule of 1-hexyne revealing a new radical anion with an increased separation distance from radical anion. These assumptions are consistent with the development of a red-brownish color at the Cu(BDC)/(Au@Si) cathode, which is typical for anion radicals.⁴³

Higher product yields are prohibited by the fact that the Cu(BDC)/(Au@Si) cathode effectively blocks charge flow through the film, and the resulting very low currents limit the amount of the produced material. To overcome this limitation, we carried out potentiostatic EP experiments in a simple two-electrode setup configuration consisting of a U-shaped glass electrolytic cell, separated into two compartments by a porous glass disk. Constant DC voltage was adjusted to the point when red-brownish color appears around the cathode and reached $-3.5 \pm 0.5 \text{ V}$.

Successful EP of the 1-hexyne monomers to yield BPA oligomers is demonstrated by the IRRAS and Raman data (Figure 2). The IR peak at 1631 cm^{-1} is characteristic for the conjugated $-C=C-$ units within PA¹⁴ and attributed to the

stretching of the alkene double bond and thus provided direct evidence of BPA formed during the reaction. Inspection of the $\sim 3000 \text{ cm}^{-1}$ region in the Raman spectra evidence strong chemical changes associated with the formation of the conjugated $-PA-$ chains: in addition to the C–H of butyl tails, a new set of sharp peaks at 2869 , 2875 , and 2781 cm^{-1} is seen (red dotted lines). The latter bands are characteristic for the $(C=C-H)$ symmetric and asymmetric stretching frequency of the conjugated polymer main chain.⁴⁴ Raman active modes between ~ 1260 and $\sim 1600 \text{ cm}^{-1}$ are well-understood features of the vibrational spectrum of *trans*-polyacetylene ($C=C$ stretching).⁴⁵ Consequently, the intensity increase of the band at 1627 cm^{-1} is attributed to the overlapping of vibrational bands of conjugated polymer main chain and the MOF. Closer inspection evidenced the presence of two weak features at ~ 1360 and $\sim 1660 \text{ cm}^{-1}$, which are attributed to doping-induced Raman bands in BPA (Figure 2a, Figure S1b, red arrows).⁴⁶

After the EP process, no further changes in the XRD diffraction peak positions were observed, only the overall intensities of the diffraction peaks were slightly reduced (Figure 2b). These observations revealed that no contraction or change in symmetry of the host framework happened upon polymerization of the guest monomers.⁴⁷ Focused ion beam (FIB) and scanning electron microscopy (SEM), combined with energy-dispersive X-ray (EDX) were used for imaging and analysis of the film (Figure S4). The results show the layered sample structure, where the MOF film appears as a dark contrast with a thickness of $100 \pm 5 \text{ nm}$ on top of the gold film with a thickness of $90 \pm 5 \text{ nm}$. The EDX analysis also reveals the presence of major amounts of Cu within the dark layer of MOF, whereas major amounts of gold were found along with stripes of the gold electrode (Figure S4). Further firm evidence for the presence of BPA was obtained by MALDI-ToF MS analysis as shown in Figure 3a. Prior to analysis, the film was dissolved by immersing the SURMOF sample into a 50% ethanolic acetic acid solution (see the [Supporting Information](#)). The resulting solution was subsequently analyzed using

MALDI-ToF MS. Considering H- and Bu-groups as terminating, $[M^+]$ was calculated as follow: $15 \cdot M[C_6H_{10}] + M[H] + M[C_4H_9] = C_{194}H_{160}$. The experimentally detected mass peak corresponds to the adduct of composition $[M^+ + 2H + Li]$. The origin of lithium can be explained by the sample preparation method. Although the presence of such “chemical noise” is widely recognized and numerous attempts have been made to reduce its effect, its nature and origins are not yet understood in detail.⁴⁸

Series of peaks are visible up to ~ 3000 Da, with the progressive decrease in the peak intensity from the strongest peak at 1299.35 Da, where the chain length observed is $n = 15$. There is a gap of 82.08 amu between adjacent peaks, consistent with a BPA repeating unit. Any other major series different to 82.08 amu mass differences are not observed, suggesting that all the polymer chains are composed of one kind of structure. The suggested EP mechanism is sketched in Figure 3b. Despite the stability of quaternary ammonium cations beyond lithium reducing potentials (nominally beyond -3.05 V vs SHE) reduction of quaternary ammonium cations should be considered^{49,50} (Figure 3b). The reduction of quaternary ammonium cations in organic solvents proceeds by an initial one-electron step with the expulsion of an alkyl carbon radical (Bu•) and consequent formation of a tertiary amine (step 1). The Bu-radical reacts with the propagated ion-radical of step 2 to form a carbanion. It is well-known that this carbanion can act as a Bronsted base abstracting a β -proton from a pristine $[N_{4444}]^+$ cation in a Hoffman elimination reaction. Thus, H- and Bu-groups are considered as terminating groups, which is in agreement with the molecular mass of the strongest peak at 1299.35 Da detected in MALDI-ToF MS and corresponds to the calculated value for $C_{94}H_{160} [M^+ + 2H + Li]$: 1299, 24. Moreover, the narrow mass distribution stands for the exclusive polymerization in the pores of the MOF.

To evaluate the effect of the in-pore EP formation of BPA chains and the electrical conductivity of the embedded polyacetylene chains, we grew the Cu(BDC) SURMOF film on interdigitated gold electrodes using layer-by-layer spray deposition.⁵¹ A film thickness of 100 nm was determined by SEM (Figure S4). X-ray diffraction (XRD) measurements (Figure S2) demonstrate the crystalline oriented film growth with the targeted Cu(BDC) structure.⁵² Current–voltage (I – V) characteristics of the pristine thin-film device (Figure 4) exhibited a very low conductivity ($\sim 6 \times 10^{-10}$ S m^{-1}), consistent with the expected insulating nature of empty Cu(BDC) SURMOF-2. Upon EP in the pores, the current increased tremendously. The I – V curve is linear, showing an ideal ohmic behavior. The fact that the host SURMOFs could also be grown on substrates with prepatterned electrodes allowed for the in situ determination of the electrical conductivity, in contrast to previous work,^{30,31} where the conductive polymer formed by electropolymerization had to be removed from the substrate and further processed before the material could be characterized. The conductivity of the PA@Cu(BDC)-SURMOF-2 sample was found to amount to 0.098 S m^{-1} . The polymerization in the pores thus increased the electrical conductivity of the sample by 8 orders of magnitude. Moreover, the observed increased conductivity is long-time stable and the I – V curve of a sample stored in argon for 3 months is virtually identical. These observations reveal that the polyacetylene chains formed in the EP process must be doped, since the pure polyacetylene is an insulator. We propose that in our case traces of Cl generated by electrolysis of the solvent

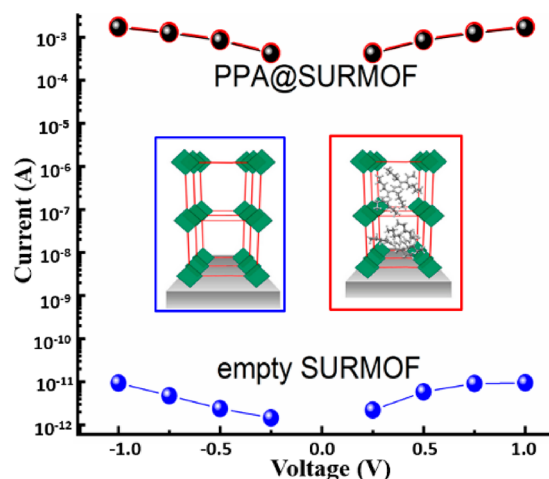


Figure 4. Current–voltage curves before (blue) and after (black) infiltration with 1-hexyne1 and EP. The red data points, virtually identical with the black points, were measured after 3 months after EP where the sample was stored in pure argon at room temperature.

cause a p-doping of the polyacetylene oligomers.⁵³ The presence of p-doping would also be consistent with the rather high stability of the compounds formed in the EP process.⁵⁴

Because in the (nonconducting) SURMOFs, polyacetylene oligomers are present rather than long, extended polymer strands (see above), the occurrence of electrical conductivity requires the percolation of the short polymer chains. The electrical conductivity of such networks depends on the charge transport within the oligomers (intrachain) and the hopping of charges from chain to chain (interchain). As the electrical conductivity of doped polyacetylene (~ 1 – 10 S m^{-1}) is much larger than the values measured for our systems, the electrical conductivity is determined only by interchain transport. According to an established percolation model,⁵⁵ in such cases, the overall conductivity is given by the interrupted bond probability⁵⁶ p , and the interchain conductivity σ_{per} . Calculations carried out for the present case (see the Supporting Information) yield $p = 26.6\%$ and $\sigma_{per} = 9.29 \times 10^{-3}$ S m^{-1} (see the Supporting Information). Using these values, we obtain an upper bound for the conductivity of our SURMOF/polymer system of 0.12 S m^{-1} , a value which is within 25% of three of the experimental values.

3. CONCLUSIONS

We have successfully carried out the cathodic electrochemical polymerization at constant DC voltage of monosubstituted alkyne monomers confined in nanochannels of surface-mounted thin films of Cu(BDC) MOF (SURMOF-2). The crystallinity of the host SURMOF substrate is not affected by the EP-process. MS analysis evidenced the progressive decrease of the peak intensity from the strongest peak at 1299.35 Da, corresponding to the chain length of $n = 15$ and is visible out to ~ 3000 Da. The formation of BPA in its trans-configuration is confirmed by spectroscopic methods. The use of a layer-by-layer process to grow the HOST MOF thin film on a prepatterned substrate allowed for the in situ determination of the electrical conductivity, which amounted to 0.1 S m^{-1} , 8 orders of magnitude greater than that of the pristine SURMOF. A theoretical analysis revealed that this conductivity is limited by hopping of electrons between the percolation network formed by the polyacetylene oligomers.

■ ASSOCIATED CONTENT

■ Supporting Information

The Supporting Information is available free of charge at <https://pubs.acs.org/doi/10.1021/acsami.0c07036>.

Experimental and computational details (PDF)

■ AUTHOR INFORMATION

Corresponding Authors

Svetlana Klyatskaya – Institute of Nanotechnology, Karlsruhe Institute of Technology, Eggenstein-Leopoldshafen 76344, Germany; orcid.org/0000-0003-2883-750X; Email: svetlana.klyatskaya@kit.edu

Mario Ruben – Institute of Nanotechnology, Karlsruhe Institute of Technology, Eggenstein-Leopoldshafen 76344, Germany; Institut de Physique et Chimie des Matériaux de Strasbourg (IPCMS), CNRS-Université de Strasbourg, Strasbourg Cedex 2 67034, France; orcid.org/0000-0002-7718-7016; Email: mario.ruben@kit.edu

Lars Heinke – Institute of Functional Interfaces (IFG), Karlsruhe Institute of Technology (KIT), Eggenstein-Leopoldshafen 76344, Germany; Email: lars.heinke@kit.edu

Authors

Anemar Bruno Kanj – Institute of Functional Interfaces (IFG), Karlsruhe Institute of Technology (KIT), Eggenstein-Leopoldshafen 76344, Germany; orcid.org/0000-0001-6385-4634

Concepción Molina-Jirón – Institute of Nanotechnology, Karlsruhe Institute of Technology, Eggenstein-Leopoldshafen 76344, Germany

Shahriar Heidrich – Institute of Nanotechnology, Karlsruhe Institute of Technology, Eggenstein-Leopoldshafen 76344, Germany; orcid.org/0000-0002-9691-4012

Leonardo Velasco – Institute of Nanotechnology, Karlsruhe Institute of Technology, Eggenstein-Leopoldshafen 76344, Germany; orcid.org/0000-0003-0151-9253

Carsten Natzeck – Institute of Functional Interfaces (IFG), Karlsruhe Institute of Technology (KIT), Eggenstein-Leopoldshafen 76344, Germany

Hartmut Gliemann – Institute of Functional Interfaces (IFG), Karlsruhe Institute of Technology (KIT), Eggenstein-Leopoldshafen 76344, Germany

Stefan Heissler – Institute of Functional Interfaces (IFG), Karlsruhe Institute of Technology (KIT), Eggenstein-Leopoldshafen 76344, Germany

Peter Weidler – Institute of Functional Interfaces (IFG), Karlsruhe Institute of Technology (KIT), Eggenstein-Leopoldshafen 76344, Germany

Wolfgang Wenzel – Institute of Nanotechnology, Karlsruhe Institute of Technology, Eggenstein-Leopoldshafen 76344, Germany

Carlos Cesar Bof Bufon – Brazilian Nanotechnology National Laboratory (LNNano), Brazilian Center for Research in Energy and Materials (CNPEM), Campinas 13083-970, São Paulo, Brazil; orcid.org/0000-0002-1493-8118

Christof Wöll – Institute of Functional Interfaces (IFG), Karlsruhe Institute of Technology (KIT), Eggenstein-Leopoldshafen 76344, Germany; orcid.org/0000-0003-1078-3304

Complete contact information is available at: <https://pubs.acs.org/doi/10.1021/acsami.0c07036>

Author Contributions

The manuscript was written through contributions of all authors. All authors have given approval to the final version of the manuscript.

Funding

This research was funded by the KIT, DFG, and CAPES.

Notes

The authors declare no competing financial interest.

■ ACKNOWLEDGMENTS

Funding by the German Research Foundation (DFG) through the priority programs 1928 COORNETs and the Excellence Cluster 3D Matter Made to Order (EXC-2082/1-390761711, Germany's Excellence Strategy) is gratefully acknowledged. We thank Dr. R. Azmi and SURMOF-Factory (ih-Proposal 2017-018-019109) for the generous support in providing the SURMOF-2 samples, TOF-SIMS analysis, and discussions. C.C.B.B. also acknowledges CAPES/Alexander von Humboldt Foundation for an Experienced Research Fellowship (CAPES Process 88881.145646/2017-01). We are also indebted to the KNMF facility (KIT, Germany) for continuous support.

■ REFERENCES

- (1) Cosnier, S.; Karyakin, A. *Electropolymerization: Concepts, Materials, and Applications*; Wiley, 2011; pp 296.
- (2) Chien, J. C. W. *Polyacetylene: Chemistry, Physics, and Material Science*; Elsevier Science, 2012; pp 648.
- (3) Shirakawa, H.; Masuda, T.; Takeda, K. In *Triple Bonded Functional Groups*; Patai, S., Ed.; John Wiley & Sons, 2004; pp 945–1016.
- (4) Bertoncello, P.; Stewart, A. J.; Dennany, L. Analytical Applications of Nanomaterials in Electrogenated chemiluminescence. *Anal. Bioanal. Chem.* **2014**, 406 (23), 5573–5587.
- (5) Salminen, K.; Groenroos, P.; Tuomi, S.; Kulmala, S. Cathodic electrogenerated chemiluminescence of Aromatic Tb(III) Chelates at Polystyrene-Graphite Composite Electrodes. *Anal. Chim. Acta* **2017**, 985, 54–60.
- (6) Rolison, D. R.; Long, J. W.; Lytle, J. C.; Fischer, A. E.; Rhodes, C. P.; McEvoy, T. M.; Bourg, M. E.; Lubers, A. M. Multifunctional 3D Nanoarchitectures for Energy Storage and Conversion. *Chem. Soc. Rev.* **2009**, 38 (1), 226–252.
- (7) Ye, L.; Liu, J.; Gao, Y.; Gong, C.; Addicoat, M.; Heine, T.; Wöll, C.; Sun, L. Highly Oriented MOF Thin Film-based Electrocatalytic Device for the Reduction of CO₂ to CO Exhibiting High Faradaic Efficiency. *J. Mater. Chem. A* **2016**, 4, 15320–15326.
- (8) Gardella, L.; Colonna, S.; Fina, A.; Monticelli, O. A Novel Electrostimulated Drug Delivery System Based on PLLA Composites Exploiting the Multiple Functions of Graphite Nanoplatelets. *ACS Appl. Mater. Interfaces* **2016**, 8 (37), 24909–24917.
- (9) Skotheim, T. A.; Reynolds, J. R. *Handbook of Conducting Polymers*, 3rd ed.; CRC Press, 2007; Vol 1, 2, pp 1680.
- (10) Balint, R.; Cassidy, N. J.; Cartmell, S. H. Conductive Polymers: Towards a Smart Biomaterial for Tissue Engineering. *Acta Biomater.* **2014**, 10 (6), 2341–2353.
- (11) Chujo, Y. *Conjugated Polymer Synthesis: Methods and Reactions*; John Wiley & Sons, 2011; pp 328.
- (12) Nalwa, H. S. *Advanced Functional Molecules and Polymers: Electronic and Photonic Properties*; CRC Press, 2001; pp 386.
- (13) Kijima, M.; Ohmura, K.; Shirakawa, H. Electrochemical Synthesis of Free-standing Polyacetylene Film with Copper Catalyst. *Synth. Met.* **1999**, 101 (1–3), 58.
- (14) Şahin, Y.; Pekmez, K.; Yildiz, A. Electrochemical Polymerization of Acetylene with Copper Catalyst on Platinum and Copper Electrodes. *Synth. Met.* **2002**, 129 (2), 117–121.

- (15) Katz, M.; Wendt, H. A Comparative Study of the Direct Anodic Oxidation of Olefins and Acetylenes in Non-aqueous Solvents. *Electrochim. Acta* **1976**, *21* (3), 215–218.
- (16) Qu, L.; Iguchi, H.; Takaishi, S.; Habib, F.; Leong, C. F.; D'Alessandro, D. M.; Yoshida, T.; Abe, H.; Nishibori, E.; Yamashita, M. Porous Molecular Conductor: Electrochemical Fabrication of Through-Space Conduction Pathways among Linear Coordination Polymers. *J. Am. Chem. Soc.* **2019**, *141* (17), 6802–6806.
- (17) Lin, R.-B.; Xiang, S.; Li, B.; Cui, Y.; Qian, G.; Zhou, W.; Chen, B. Our Journey of Developing Multifunctional Metal-organic Frameworks. *Coord. Chem. Rev.* **2019**, *384*, 21–36.
- (18) Stavila, V.; Talin, A. A.; Allendorf, M. D. MOF-based Electronic and Opto-electronic Devices. *Chem. Soc. Rev.* **2014**, *43*, 5994–6010.
- (19) Stassen, I.; Burtch, N.; Talin, A.; Falcato, P.; Allendorf, M.; Ameloot, R. An Updated Roadmap for the Integration of Metal-organic Frameworks with Electronic Devices and Chemical Sensors. *Chem. Soc. Rev.* **2017**, *46*, 3185–3241.
- (20) Liu, J.; Wöll, C. Surface-supported Metal-organic Framework Thin Films: Fabrication Methods, Applications, and Challenges. *Chem. Soc. Rev.* **2017**, *46*, 5730–5770.
- (21) Sun, L.; Campbell, M. G.; Dincă, M. Electrically Conductive Porous Metal-Organic Frameworks. *Angew. Chem., Int. Ed.* **2016**, *55* (11), 3566–3579.
- (22) Dragässer, A.; Shekhah, O.; Zybaylo, O.; Shen, C.; Buck, M.; Wöll, C.; Schlottwein, D. Redox Mediation Enabled by Immobilised Centres in the Pores of a Metal-organic Framework Grown by Liquid Phase Epitaxy. *Chem. Commun.* **2012**, *48*, 663–665.
- (23) Talin, A. A.; Centrone, A.; Ford, A. C.; Foster, M. E.; Stavila, V.; Haney, P.; Kinney, A.; Szalai, V.; El Gabaly, F.; Yoon, H. P.; Léonard, F.; Allendorf, M. D. Tunable Electrical Conductivity in Metal-Organic Framework Thin-Film Devices. *Science* **2014**, *343* (6166), 66–69.
- (24) Dhara, B.; Nagarkar, S. S.; Kumar, J.; Kumar, V.; Jha, P. K.; Ghosh, S. K.; Nair, S.; Ballav, N. Increase in Electrical Conductivity of MOF to Billion-Fold upon Filling the Nanochannels with Conducting Polymer. *J. Phys. Chem. Lett.* **2016**, *7* (15), 2945–2950.
- (25) Le Ouay, B.; Boudot, M.; Kitao, T.; Yanagida, T.; Kitagawa, S.; Uemura, T. Nanostructuring of PEDOT in Porous Coordination Polymers for Tunable Porosity and Conductivity. *J. Am. Chem. Soc.* **2016**, *138* (32), 10088–10091.
- (26) Uemura, T.; Yanai, N.; Kitagawa, S. Polymerization Reactions in Porous Coordination Polymers. *Chem. Soc. Rev.* **2009**, *38*, 1228–1236.
- (27) Hassan, M. H.; Haikal, R. R.; Hashem, T.; Rinck, J.; Koeniger, F.; Thissen, P.; Stefan Heißler; Woll, C.; Alkordi, M. H. Electrically Conductive, Monolithic Metal-Organic Framework-Graphene (MOF@G) Composite Coatings. *ACS Appl. Mater. Interfaces* **2019**, *11* (6), 6442–6447.
- (28) Kung, C.-W.; Han, P.-C.; Chuang, C.-H.; Wu, K. C.-W. Electronically Conductive Metal-Organic Framework-Based Materials. *APL Mater.* **2019**, *7*, 110902.
- (29) Haldar, R.; Sen, B.; Hurtle, S.; Kitao, T.; Sankhla, R.; Kühl, B.; Welle, A.; Heissler, S.; Brenner-Weiß, G.; Thissen, P.; Uemura, T.; Gliemann, H.; Barner-Kowollik, C.; Wöll, C. Oxidative Polymerization of Terthiophene and a Substituted Thiophene Monomer in Metal-Organic Framework Thin Films. *Eur. Polym. J.* **2018**, *109*, 162–168.
- (30) Uemura, T.; Yanai, N.; Kitagawa, S. Polymerization Reactions in Porous Coordination Polymers. *Chem. Soc. Rev.* **2009**, *38*, 1228–1236.
- (31) Uemura, T.; Kitaura, R.; Ohta, Y.; Nagaoka, M.; Kitagawa, S. Nanochannel-Promoted Polymerization of Substituted Acetylenes in Porous Coordination Polymers. *Angew. Chem.* **2006**, *118* (25), 4218–4222.
- (32) Lu, C.; Ben, T.; Xu, S.; Qiu, S. Electrochemical synthesis of a Microporous Conductive Polymer Based on a Metal-Organic Framework Thin Film. *Angew. Chem., Int. Ed.* **2014**, *53* (25), 6454–6458.
- (33) Chiang, C. K.; Fincher, C. R.; Park, Y. W.; Heeger, A. J.; Shirakawa, H.; Louis, E. J.; Gau, S. C.; MacDiarmid, A. G. Electrical Conductivity in Doped Polyacetylene. *Phys. Rev. Lett.* **1977**, *39* (17), 1098–1101.
- (34) Wang, S.; Feng, X.; Zhao, Z.; Zhang, J.; Wan, X. Reversible *Cis-Cisoid* to *Cis-Transoid* Helical Structure Transition in Poly(3,5-disubstituted phenylacetylene)s. *Macromolecules* **2016**, *49*, 8407–8417.
- (35) Motoshige, A.; Mawatari, Y.; Yoshida, Y.; Motoshige, R.; Tabata, M. Synthesis and Solid State *Helix* to *Helix* Rearrangement of Poly(phenylacetylene) Bearing *n*-Octyl Alkyl Side Chains. *Polym. Chem.* **2014**, *5*, 971–978.
- (36) Mawatari, Y.; Tabata, M. Carbon-Related Materials. In *Recognition of Nobel Lectures by Prof. Akira Suzuki ICCE*; Kaneko, S., Mele, P., Endo, T., Tsuchiya, T., Tanaka, K., Eds.; Springer International Publishing, 2017; pp457.
- (37) Albano, L. G. S.; Vello, T. P.; de Camargo, D. H. S.; da Silva, R. M. L.; Padilha, A. C. M.; Fazzio, A.; Bufon, C. C. B. Ambipolar Resistive Switching in an Ultrathin Surface-Supported Metal-Organic Framework Vertical Heterojunction. *Nano Lett.* **2020**, *20* (2), 1080–1088.
- (38) Liu, J.; Lukose, B.; Shekhah, O.; Arslan, H. K.; Weidler, P.; Gliemann, H.; Bräse, S.; Grosjean, S.; Godt, A.; Feng, X.; Müllen, K.; Magdau, I.-B.; Heine, T.; Wöll, C. A Novel Series of Isorecticular Metal Organic Frameworks: Realizing Metastable Structures by Liquid Phase Epitaxy. *Sci. Rep.* **2012**, *2*, 921.
- (39) Shekhah, O.; Wang, H.; Kowarik, S.; Schreiber, F.; Paulus, M.; Tolan, M.; Sternemann, C.; Evers, F.; Zacher, D.; Fischer, R. A.; Wöll, C. Step-by-Step Route for the Synthesis of Metal-Organic Frameworks. *J. Am. Chem. Soc.* **2007**, *129* (49), 15118–15119.
- (40) Heinke, L.; Wöll, C. Surface-Mounted Metal-Organic Frameworks: Crystalline and Porous Molecular Assemblies for Fundamental Insights and Advanced Applications. *Adv. Mater.* **2019**, *31* (26), 1806324.
- (41) Kennedy, D. C.; McKay, C. S.; Tay, L.; Rouleau, Y.; Pezacki, J. P. Carbon-Bonded Silver Nanoparticles: alkyne-Functionalized Ligands for SERS Imaging of Mammalian Cells. *Chem. Commun.* **2011**, *47*, 3156–3158.
- (42) Yoo, B. K.; Joo, S. W. In Situ Raman Monitoring Triazole Formation From Self-assembled Monolayers of 1,4-Diethynylbenzene on Ag and Au Surfaces via “Click” Cyclization. *J. Colloid Interface Sci.* **2007**, *311* (2), 491–496.
- (43) Jakubowski, J. J.; Subramanian, R. V. Electroinitiated Polymerization and Copolymerization of Phenylacetylene. *Polym. Bull.* **1979**, *1*, 785–791.
- (44) Adams, W.; Sonntag, M. D. Vibrational Spectroscopy of Hexynes: A Combined Experimental and Computational Laboratory Experiment. *J. Chem. Educ.* **2018**, *95* (7), 1205–1210.
- (45) MacInnes, D., jr.; Druy, M. A.; Nigrey, P. J.; Nairns, D. P.; MacDiarmid, A. G.; Heeger, A. J. Organic Batteries: Reversible *n*- and *p*- Type Electrochemical Doping of Polyacetylene, (CH)_x. *J. Chem. Soc., Chem. Commun.* **1981**, 317–319.
- (46) Kim, J.-Y.; Kim, E.-R.; Ihm, D.-W.; Tasumi, M. Relationships between the Raman Excitation Photon Energies and Its Wavenumbers in Doped trans-Polyacetylene. *Bull. Korean Chem. Soc.* **2002**, *23* (10), 1404–1408.
- (47) Heck, R.; Shekhah, O.; Zybaylo, O.; Weidler, P. G.; Friedrich, F.; Maul, R.; Wenzel, W.; Wöll, C. Loading of Two Related Metal-Organic Frameworks (MOFs), [Cu₂(bdc)₂(dabco)] and [Cu₂(ndc)₂(dabco)], with Ferrocene. *Polymers* **2011**, *3* (3), 1565–1574.
- (48) Krutchinsky, A. N.; Chait, B. T. On the Mature of the Chemical Noise in MALDI Mass Spectra. *J. Am. Soc. Mass Spectrom.* **2002**, *13*, 129–134.
- (49) Luca, O. R.; Gustafson, J. L.; Maddox, S. M.; Fenwick, A. Q.; Smith, D. C. Catalysis by Electrons and Holes: Formal Potential Scales and Preparative Organic Electrochemistry. *Org. Chem. Front.* **2015**, *2*, 823–848.

(50) Lane, G. H. Electrochemical Reduction Mechanisms and Stabilities of Some Cation Types Used in Ionic Liquids and Other Organic Salts. *Electrochim. Acta* **2012**, 83 (30), 513–528.

(51) Hurrele, S.; Friebe, S.; Wohlgemuth, J.; Woll, C.; Caro, J.; Heinke, L. Sprayable, Large-Area MOF Films and Membranes of Varying Thickness. *Chem. - Eur. J.* **2017**, 23, 2294–2298.

(52) Friedländer, S.; Liu, J.; Addicoat, M.; Petkov, P.; Vankova, N.; Rüger, R.; Kuc, A.; Guo, W.; Zhou, W.; Lukose, B.; Wang, Z.; Weidler, P. G.; Pöppel, A.; Ziese, M.; Heine, T.; Wöll, C. Linear Chains of Magnetic Ions Stacked with Variable Distance: Ferromagnetic Ordering with a Curie Temperature above 20 K. *Angew. Chem., Int. Ed.* **2016**, 55 (41), 12683–12687.

(53) Kotsinakis, A.; Kyriacou, G.; Lambrou, Ch. Electrochemical Reduction of Dichloromethane to Higher Hydrocarbons. *J. Appl. Electrochem.* **1998**, 28 (6), 613–619.

(54) Saxman, M.; Liepins, R.; Aldissi, M. Polyacetylene: Its Synthesis, Doping and Structure. *Prog. Polym. Sci.* **1985**, 11 (1–2), 57–89.

(55) Cottaar, J.; Koster, L. J. A.; Coehoorn, R.; Bobbert, P. A. Scaling Theory for Percolative Charge Transport in Disordered Molecular Semiconductors. *Phys. Rev. Lett.* **2011**, 107 (13), 136601.

(56) Shirakawa, H.; Louis, E. J.; MacDiarmid, A. G.; Chiang, C. K.; Heeger, A. J. Synthesis of Electrically Conducting Organic Polymers: Halogen Derivatives of Polyacetylene, $(CH)_x$. *J. Chem. Soc., Chem. Commun.* **1977**, 578–580.